THE JOURNAL OF PHYSICAL CHEMISTRY C

Article

pubs.acs.org/JPCC

Structural Origins of Potential Dependent Hysteresis at the Electrified Graphene/Ionic Liquid Interface

Ahmet Uysal,*[,†] Hua Zhou,[‡] Guang Feng,*[,§] Sang Soo Lee,[†] Song Li,[§] Paul Fenter,*[,†] Peter T. Cummings,[§] Pasquale F. Fulvio,[∥] Sheng Dai,[∥] John K. McDonough,[⊥] and Yury Gogotsi[⊥]

[†]Chemical Science and Engineering Division and [‡]Advanced Photon Source, Argonne National Laboratory, Argonne, Ilinois 60439, United States

[§]Department of Chemical and Biomolecular Engineering, Vanderbilt University, Nashville, Tennessee 37235, United States

[∥]Chemical Science Division, Oak Ridge National Laboratory, Oak Ridge, Tennessee 37831, United States

[⊥]Department of Materials Science and Engineering and A.J. Drexel Nanotechnology Institute, Drexel University, Philadelphia, Pennsylvania 19104, United States

ABSTRACT: We studied the potential and time-dependent changes in the electric double layer (EDL) structure of an imidazolium-based room temperature ionic liquid (RTIL) electrolyte at an epitaxial graphene (EG) surface. We used in situ X-ray reflectivity (XR) to determine the EDL structure at static potentials, during cyclic voltammetry (CV) and potential step measurements. The static potential structures were also investigated with fully atomistic molecular dynamics (MD) simulations. Combined XR and MD results show that the EDL structure has alternating anion/cation layers within the first nanometer of the interface and that these structures are distinct at the most positive and negative static potentials (1.0 and −0.4 V, respectively) applied in this study. The dynamical response of the EDL to potential steps has a slow component (>10 s) and the RTIL structure shows hysteresis during CV scans (e.g., at 100 mV/s scan rate). Our results reveal that both the slow kinetics and hysteresis are due to the reorganization of the distinct EDL structures found at the extreme potentials.

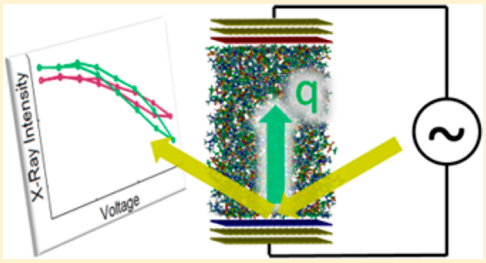

1. INTRODUCTION

Electrical double layer capacitors (EDLCs) with room temperature ionic liquid (RTIL) electrolytes and carbon electrodes are promising candidates for energy storage devices with high power density and long cycle life.[1−3] A fundamental understanding of RTIL-based EDLCs requires a well-defined relationship between the nanoscale interfacial structure and the applied electrochemical conditions. RTIL/electrode interfaces have become the subject of various theoretical,[4−6] computational,[7−12] and experimental[13−29] studies. Multiple recent experiments have revealed an unexpectedly slow RTIL response[17−20] as well as hysteretic behavior[23−28] in differential capacitance (DC) measurements. Hysteresis in the DC-potential data was first observed in electrochemical impedance spectroscopy (EIS)[22−25] experiments. Sum frequency generation (SFG),[27] surface plasmon resonance (SPR),[17] and surface-enhanced infrared absorption spectroscopy (SEIRAS)[28] measurements also showed hysteretic effects at RTIL/electrode interfaces. Similarly, slow capacitive processes were discovered in EIS[19−21] and confirmed by SPR measurements.[17] Clearly, a more direct understanding of the actual, real time, interfacial RTIL structure under electrochemical control is needed.

In situ X-ray reflectivity (XR) is a powerful, contact-free method to study liquid−solid interfaces.[30−38] It probes the interfacial structures of both the liquid and the solid directly, with subnanometer structural resolution, especially when integrated with theoretical and computational methods.[32−34] Only a few X-ray studies of RTIL/charged interfaces have been reported.[30−32] One of the main observations from these measurements is the presence of strong cation−anion layering near charged interfaces. Also, the first RTIL layer of $[bmim^+][Tf_2N^-]$ at the neutral EG and the negatively charged muscovite mica surfaces was found to form a distinct "adsorbed" layer,[32] as suggested by AFM force curve measurements.[39] Interestingly, no density enhancement was observed for the first adsorbed RTIL layer at a sapphire surface,[30] whose charge was not intrinsic but assumed to be induced by the X-ray radiation, suggesting that this system may not be representative of RTILs at charged electrodes.

We use epitaxial graphene (EG) as a model electrode for the electrolyte−carbon interface. It is atomically flat and therefore is ideally suited for XR measurements. Furthermore, graphene based electrodes have been suggested as an alternative to porous carbon materials for supercapacitor applications because of their low resistivity.[40,41]

In this manuscript, we present in situ X-ray scattering experiments that probe the static and dynamic interfacial structures of $[C_9mim^+][Tf_2N^-]$ ionic liquid at EG electrodes

Received: November 11, 2013
Revised: December 6, 2013
Published: December 10, 2013

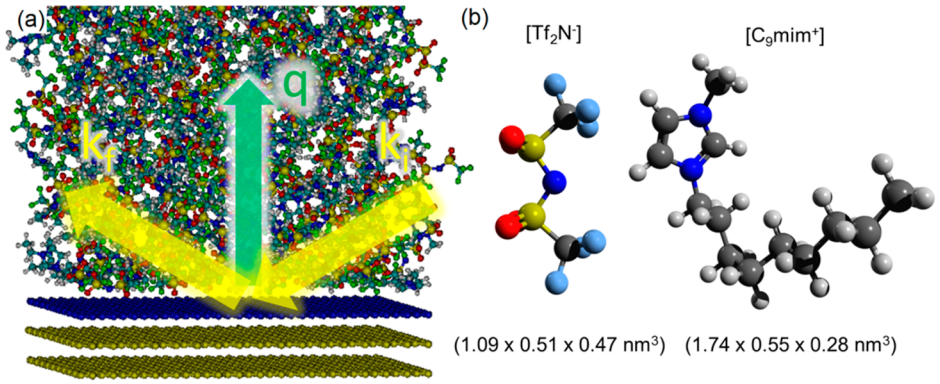

Figure 1. (a) Scattering geometry of the in situ specular XR measurement as a function of the vertical momentum transfer ($q = k_f - k_i$) is depicted with an MD simulation snapshot. (b) Molecular models of [Tf_2N^-] and [C_9mim^+] ions.

under applied potentials and during cyclic voltammetry and potential step measurements. Parallel classical molecular dynamics (MD) simulations were performed to obtain molecular-scale information about RTIL−graphene interface structures under different static potentials. Figure 1a shows an illustration of the specular XR geometry with a snapshot from an actual MD simulation. The results reveal potential dependent hysteresis in CV scans and a slow process during potential steps that are associated with reorganization of the interfacial RTIL structure, and suggest that both hysteresis and slow process may be originating from the same mechanism.

2. EXPERIMENTAL AND COMPUTATIONAL DETAILS

2.1. In Situ X-ray Scattering Experiments. A custom-made transmission sample cell, similar to a previously described design,[42] with a Pt counter electrode and a Pt pseudo reference electrode was controlled by Gamry Reference-600 potentiostat. A 10 × 3 × 0.5 mm^3 sample, used as a working electrode, was contacted from both ends of the surface by two connectors insulated by Kel-F shells. The sample thickness along the incident X-ray beam direction was 3 mm. X-ray scattering experiments were conducted at Sectors 33-IDD, 12-IDD, and 6-IDB of Advanced Photon Source. The monochromatic X-ray photon energy was 20 keV (λ = 0.62 Å) and the incidence beam dimensions were set to ∼80 μm vertically and ∼1 mm horizontally. The specular XR signal was measured as a function of vertical momentum transfer $q = k_f - k_i = (4\pi/\lambda)\sin(2\theta/2)$ (Figure 1a). Details of similar liquid−solid interface X-ray scattering experiments had been published previously.[32,33,43]

2.2. Epitaxial Graphene Growth. 6H (0001) SiC wafers (n-doped) were purchased form Cree Inc. Epitaxial graphene was grown on Si-terminated faces by thermal decomposition in an MTI GSL1700X tube furnace under argon environment[44] (600−900 mbar) at 1550 °C.

2.3. 1-Methyl-3-nonylimidazolium Bis-(trifluoromethanesulfonyl)imide [C_9mim^+][Tf_2N^-] RTIL Synthesis. A 250 mL round-bottom flask was charged with 125 mL of ethyl acetate, 0.20 mol of 1-methyl-imidazole (Sigma Aldrich), and 0.20 mol of 1-bromononane (Sigma Aldrich). The solution was stirred under argon for 72 h. The organic liquid phase formed was separated and thoroughly washed with ethyl acetate and reacted with an aqueous solution having 1 equiv of lithium bis(trifluoromethanesulfonyl)imide (3 M). The system was washed with ethyl acetate and water several times, and the aqueous phase was discarded after each wash. The organic phase was dried with magnesium sulfate, filtered, and the solvent was removed using a rotary evaporator for 1 h at room temperature and 1 h at 80 °C. The obtained product was finally kept in a freeze drier for several days yielding a viscous colorless liquid.

2.4. MD Simulations. We performed classical molecular dynamics (MD) simulations to obtain the molecular-scale information of interfaces between ILs and the neutral/charged graphene electrodes. The simulation was set by ILs enclosed between two electrodes with opposite charges, and each electrode was modeled as three static layers of graphene sheets. Small partial charges were placed on a plane 0.07 nm away from the geometrical plane of electrode surface (contacting with ILs) to produce a surface charge density (σ) ranging from 0.00 ± 0.01 to ±0.15 C/m^2.[45] The plane on which the surface charge is located is considered as the surface of the electrode and the lower plane is chosen as z = 0 for the coordinate system. The size of electrode vertical to z-direction is about 5.54 × 5.66 nm^2, and the separation between the opposing electrode surfaces was set as 8.0 nm to ensure the electrolyte with a bulk-like behavior adopted in the central portion of the system. Periodic boundary conditions were applied in the directions parallel to the electrodes and the simulation box size in z-direction was fixed to a value four times larger than the separation between the two electrodes. The force fields for the ions and the electrode atoms (carbon) were taken from ref 47.

Simulations were performed in the NVT ensemble using a customized MD code based on the GROMACS software.[47] The electrolyte temperature was maintained at 333 K using the Berendsen thermostat. The electrostatic interactions were computed using the PME method.[48] Specifically, an FFT grid spacing of 0.10 nm and cubic interpolation for charge distribution were used to compute the electrostatic interactions in reciprocal space. A cutoff distance of 1.2 nm was used in the calculation of electrostatic interactions in the real space. The nonelectrostatic interactions were computed by direct summation with a cutoff length of 1.2 nm. The LINCS algorithm[49] was used to maintain the bond length of the [C_9mim^+] and [Tf_2N^-] ions. Each simulation was started at 1000 K, and the simulation temperature was decreased gradually to 333 K in 6 ns. Following the annealing, the system was simulated at 333 K for 9 ns to reach equilibrium. Finally, a 9 ns production run was performed to collect the data. The potential drop across each EDL was obtained by computing the potential distribution between electrodes using the method in ref 9.

dx.doi.org/10.1021/jp4111025 | J. Phys. Chem. C 2014, 118, 569−574

3. RESULTS AND DISCUSSION

3.1. Static Potential Measurements. The X-ray reflectivity (XR) data (i.e., specular reflectivity as a function of momentum transfer, q) at −0.4 and 1.0 V fixed potentials and the best fits obtained by model dependent analysis are shown in Figure 2a. The broad peak at $q \sim 1.8$ Å^{-1} is a signature of few-layer graphene, and does not change with the applied potential, revealing that the graphene structure is stable against electrical polarization. However, the minimum near $q = 0.3$ Å^{-1} becomes more pronounced at higher potential (Figure 2a, inset). These data were understood with a structural model that uses two separate Gaussian layers close to the EG surface to simulate adsorbed layers and a distorted layered liquid (DLL) model[36,50] to describe the diffuse RTIL layers.

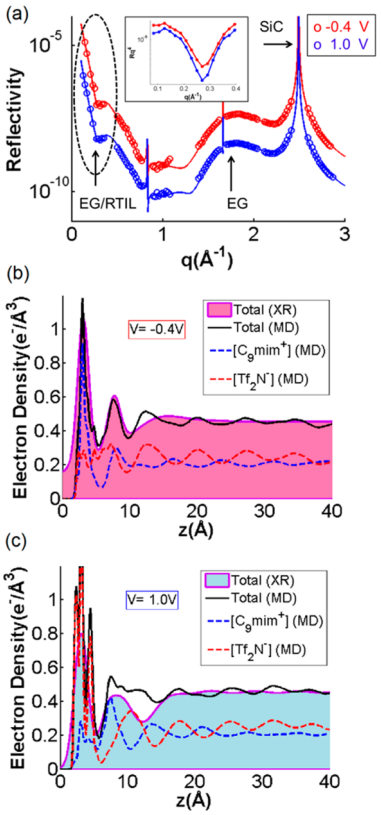

Figure 2. (a) XR data (symbols) and best fits (lines), at potentials of −0.4 and 1.0 V, based on a distorted layered liquid (DLL) model with two distinct adsorbed layers. The −0.4 V data are scaled by a decade for clarity. The inset shows the reflectivity curves multiplied by q^4 without any scaling. (b, c) Derived electron density profiles (EDPs) for [C_9mim$^+$][Tf_2N^-], at −0.4 and 1.0 V static potentials, respectively, as a function of height (z) from the EG surface, compared to those obtained independently from MD simulations.

The derived RTIL electron density profiles (EDPs; Figure 2b,c) show that the changes near $q = 0.3$ Å^{-1} are, indeed, caused mostly by structural changes in the adsorbed layer (expressed with two Gaussian peaks in the model structure). As depicted in Figure 2b,c, the total EDPs obtained by MD are validated through their correspondence with the XR results in terms of the positions and relative occupancies of the adsorbed RTIL layers, and provide additional information about the cation/anion ordering. The width of the first adsorbed layer at −0.4 V (~3.5 Å; Figure 2b) show that the imidazolium rings of the cation as well as the alkyl tails prefer to lie parallel to the graphene surface. On the other hand, the anions may have two different orientations in the first adsorbed layer at 1.0 V and cause multiple sharp peaks in the EDP (Figure 2c). The anion−cation layered structures we observe at −0.4 and 1.0 V are consistent with the previous measurements of a similar type of RTIL ([bmim$^+$][Tf_2N^-]) on uncharged graphene and negatively charged mica.[32] Our MD results also suggest that the first adsorbed layer overscreens[4] the surface charge and attracts counterions to the second layer. These two distinct layered structures suggest that extensive reorganization is likely required in the potential-driven evolution between these two extreme potential structures.

These extreme potential structures provide a context for understanding the nature of ion−ion correlations in RTILs, which have been the subject of discussion recently.[14,51,52] The derived density profiles are in good agreement with our previous XR results of RTIL structures at the charged muscovite surface, which show the presence of overcompensation of the surface charge and which was found to be consistent with theoretical predictions by Bazant et al.[4] In contrast, Gebbie et al.,[14] using a surface force apparatus, suggested that RTILs behave like dilute electrolytes with less than 0.1% dissociated ion concentrations at room temperature. However, the Derjaguin−Landau−Verwey−Overbeek (DLVO) theory they used to model their experimental data assumes a constant dielectric constant throughout the liquid, which is unlikely within the first nanometer of the charged interface. In fact, Gebbie et al. acknowledge that DLVO theory cannot be sufficient to describe that region. The first nanometer of the interfacial region is where our XR method is most sensitive and in very good agreement with MD results. Therefore, further studies that cover both regions are required.

3.2. Cyclic Voltammetry and Potential Step Measurements. Real-time XR data during CV scans (Figure 3a) were measured in the time-domain, $R(q_o,t)$, for multiple cycles with the detector and sample at fixed q_o. The intensity variation with time at $q_o = 0.3$ Å^{-1} during a CV measurement at 100 mV/s rate is shown in Figure 3b. This time scan shows an oscillatory intensity variation with a regular periodicity each of which corresponds to one CV cycle. The presented reproducibility of the data indicates that the process is reversible and the system was stable under the X-ray beam during the relevant time scales.

The voltage dependence of the EDL structure was probed by $R(V)$ curves at fixed q values. Figure 3c shows an example at $q_o = 0.3$ Å^{-1}. Since the reflectivity directly probes the interfacial structure, the presence of a path-dependent signal strength in these data directly reveals hysteresis in the interfacial RTIL *structure* during potential cycling, consistent with previous EIS,[23] SFG,[27] SPR,[17] and SERIAS[28] measurements on metal electrodes. It has been suggested that a slower scan rate reduces the magnitude in hysteresis in differential capacitance versus potential curves measured by EIS.[22] To test this hypothesis, we repeated the same measurements but at a slower scan rate (5 mV/s). Interestingly, the hysteresis became more pronounced at this slower rate (Figure 3c).

The $R(V)$ signal does not change significantly below 0 V, which is consistent with our XR measurements at this potential (not shown) that produce an XR curve that is, within experimental error, identical to the one measured at −0.4 V (Figure 2b). Principally, the imidazolium rings of cations (Figure 1b) are attracted to the graphene surface via $\pi-\pi$ interactions even when no potential is applied. Therefore,

dx.doi.org/10.1021/jp4111025 | J. Phys. Chem. C 2014, 118, 569−574

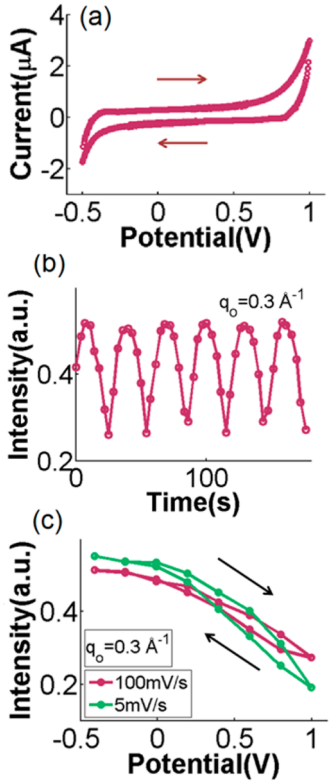

Figure 3. (a) CV data collected simultaneously with the XR measurements at 100 mV/s scan rate with 5 mV steps. (b) Real-time oscillations of the XR intensity at q = 0.3 Å^{-1} during a CV scan. (c) Real-time reflectivity data from (b) are plotted against the applied potential (a similar curve obtained at 5 mV/s rate is also shown for comparison).

applying a negative potential cannot bring more cations closer to the surface.

Potential step measurements were conducted to determine the number of processes and their rates during the transition of the EDL structure. Starting at one extreme voltage (1 or −0.4 V), the potential was switched (at t_s) to the other extreme potential (Figure 4). The time-dependent intensity (measured

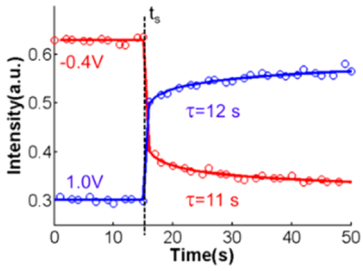

Figure 4. Potential step measurements at t_s, measured at q = 0.3 Å^{-1}. The applied potential is switched between two extreme potentials: −0.4 to 1 V (red) or 1 to −0.4 V (blue).

at q = 0.3 Å^{-1}) probes the structural changes in real time. The results show that the interfacial structure evolves by at least two different processes. We used a double exponential function to represent the fast and the slow relaxations. The fast process happens much quicker than our time resolution for X-ray measurements (∼ 1 s). However, the slow process has a time constant (τ) of around 10 s (much longer than the ∼5 ms RC constant of the system) and can be determined unambiguously. The observation of these long relaxation time constants is consistent with those from the recent spectroscopy studies[17,26] of other ionic liquids on metal electrodes. However, in contrast to the spectroscopy measurements, these time constants do not show a significant dependence on the step direction.

Our results are directly relevant to test various hypotheses in the literature about the origin of slow processes and hysteresis effects at the RTIL/electrode interface. It has been suggested that the slow processes are associated with the potential-dependent changes of the electrode surface structure.[20−22] This interpretation was possible because the working electrodes used in previous studies were metals (Pt or Au)[17,20,23−26,53] that are known to exhibit surface reconstruction above a critical surface charge.[35] However, the graphene used here is extremely stable and no surface reconstructions are known or expected. These results therefore suggest that the observed hysteresis is a property of the ionic liquids at the interfaces. A second hypothesis is that molecular conformations are responsible,[19] but as we described in the previous section, the static EDPs (Figure 2b,c) show that a change in the EDL layering structure is required as the potential changed from negative to positive or vice versa. Therefore the observed slow response cannot be explained by only rotation of molecules within a layer.

The observed hysteresis during potential cycling (Figure 3c) and the slow potential step kinetics (Figure 4) appear to be a result of steric hindrance during RTIL reorganization. These results suggest that an effective energy barrier between the two distinct structures at extreme potentials leads to an inherently slow response to the potential changes. Similar models have been suggested[28] to explain the observed hysteresis in spectroscopy measurements. It is apparent that the temporal response of the RTIL structure is inherently slow (∼seconds). However, the nature of this apparent barrier and the associated mechanism for reorganization require further investigation.

4. CONCLUSION

The EDL structure of a room temperature ionic liquid at a charged epitaxial graphene interface was understood using in situ X-ray reflectivity and MD simulations. The static potential measurements show two distinct layered structures at the most positive (1.0 V) and negative potentials (−0.4 V). The combined simulation-experiment approach provides a clear picture of the static potential EDL structure, with separated anion/cation layers. Real-time measurements show that the average *interfacial structure* responds to the applied potential slowly (>10 s) and in a path-dependent manner, as manifested by structural hysteresis. These behaviors probably originate from the distinct, layered interfacial structures at high and low potentials and reveal the relationships between the molecular interfacial structures and macroscopic properties of the RTILs, which are crucial to design RTILs with specific properties.

AUTHOR INFORMATION

Corresponding Author

*E-mail: ahmet@anl.gov (A.U.); guang.feng@vanderbilt.edu (G.F.); fenter@anl.gov (P.F.).

Notes

The authors declare no competing financial interest.

■ ACKNOWLEDGMENTS

We thank Tim T. Fister, Francesco Bellucci, and Nouamane Laanait for technical and intellectual support at various stages of the experiments. This material is based on work supported as part of the Fluid Interface Reactions, Structures and Transport (FIRST) Center, an Energy Frontier Research Center funded by the U.S. Department of Energy (DOE), Office of Science (SC), Office of Basic Energy Sciences (BES). Use of the beamlines 6ID, 12ID, and 33ID at the Advanced Photon Source was supported by DOE-SC-BES under Contract DE-AC02-06CH11357 to UChicago Argonne, LLC, as operator of Argonne National Laboratory. This research used resources of the National Energy Research Scientific Computing Center, which is supported by DOE-SC under Contract No. DE-AC02-05CH11231, and the Palmetto cluster at Clemson University.

■ REFERENCES

(1) Simon, P.; Gogotsi, Y. Capacitive energy storage in nanostructured carbon−electrolyte systems. *Acc. Chem. Res.* **2012**, *46*, 1094.
(2) Richey, F. W.; Dyatkin, B.; Gogotsi, Y.; Elabd, Y. A. Ion dynamics in porous carbon electrodes in supercapacitors using in situ infrared spectroelectrochemistry. *J. Am. Chem. Soc.* **2013**, *135*, 12818.
(3) Béguin, F.; Frackowiak, E. *Carbon Materials for Electrochemical Energy Storage Systems*. CRC: Boca Raton, FL, 2009.
(4) Bazant, M. Z.; Storey, B. D.; Kornyshev, A. A. Double layer in ionic liquids: Overscreening versus crowding. *Phys. Rev. Lett.* **2011**, *106*, 046102.
(5) Kornyshev, A. A. Double-layer in ionic liquids: paradigm change? *J. Phys. Chem. B* **2007**, *111*, 5545.
(6) Zhao, H. Diffuse-charge dynamics of ionic liquids in electrochemical systems. *Phys. Rev. E* **2011**, *84*, 051504.
(7) Vatamanu, J.; Borodin, O.; Smith, G. D. Molecular insights into the potential and temperature dependences of the differential capacitance of a room-temperature ionic liquid at graphite electrodes. *J. Am. Chem. Soc.* **2010**, *132*, 14825.
(8) Rogers, G. W.; Liu, J. Z. Graphene actuators: quantum-mechanical and electrostatic double-layer effects. *J. Am. Chem. Soc.* **2011**, *133*, 10858.
(9) Feng, G.; Zhang, J. S.; Qiao, R. Microstructure and capacitance of the electrical double layers at the interface of ionic liquids and planar electrodes. *J. Phys. Chem. C* **2009**, *113*, 4549.
(10) Lynden-Bell, R. M.; Del Popolo, M. G.; Youngs, T. G.; Kohanoff, J.; Hanke, C. G.; Harper, J. B.; Pinilla, C. C. Simulations of ionic liquids, solutions, and surfaces. *Acc. Chem. Res.* **2007**, *40*, 1138.
(11) Merlet, C.; Rotenberg, B.; Madden, P. A.; Salanne, M. Computer simulations of ionic liquids at electrochemical interfaces. *Phys. Chem. Chem. Phys.* **2013**, *15*, 15781.
(12) Vatamanu, J.; Borodin, O.; Smith, G. D. Molecular simulations of the electric double layer structure, differential capacitance, and charging kinetics for *N*-methyl-*N*-propylpyrrolidinium bis-(fluorosulfonyl)imide at graphite electrodes. *J. Phys. Chem. B* **2011**, *115*, 3073.
(13) Wang, H.; Köster, T. K. J.; Trease, N. M.; Ségalini, J.; Taberna, P.-L.; Simon, P.; Gogotsi, Y.; Grey, C. P. Real-time NMR studies of electrochemical double-layer capacitors. *J. Am. Chem. Soc.* **2011**, *133*, 19270.
(14) Gebbie, M. A.; Valtiner, M.; Banquy, X.; Fox, E. T.; Henderson, W. A.; Israelachvili, J. N. Ionic liquids behave as dilute electrolyte solutions. *Proc. Natl. Acad. Sci. U.S.A.* **2013**, *110*, 9674.
(15) Baldelli, S. Surface structure at the ionic liquid−electrified metal interface. *Acc. Chem. Res.* **2008**, *41*, 421.
(16) Lauw, Y.; Horne, M. D.; Rodopoulos, T.; Lockett, V.; Akgun, B.; Hamilton, W. A.; Nelson, A. R. Structure of [C4mpyr][NTf2] room-temperature ionic liquid at charged gold interfaces. *Langmuir* **2012**, *28*, 7374.
(17) Nishi, N.; Hirano, Y.; Motokawa, T.; Kakiuchi, T. Ultraslow relaxation of the structure at the ionic liquid‖ gold electrode interface to a potential step probed by electrochemical surface plasmon resonance measurements: asymmetry of the relaxation time to the potential-step direction. *Phys. Chem. Chem. Phys.* **2013**, *15*, 11615.
(18) Makino, S.; Kitazumi, Y.; Nishi, N.; Kakiuchi, T. Charging current probing of the slow relaxation of the ionic liquid double layer at the Pt electrode. *Electrochem. Commun.* **2011**, *13*, 1365.
(19) Roling, B.; Drüschler, M.; Huber, B. Slow and fast capacitive process taking place at the ionic liquid/electrode interface. *Faraday Discuss.* **2012**, *154*, 303.
(20) Drüschler, M.; Borisenko, N.; Wallauer, J.; Winter, C.; Huber, B.; Endres, F.; Roling, B. New insights into the interface between a single-crystalline metal electrode and an extremely pure ionic liquid: slow interfacial processes and the influence of temperature on interfacial dynamics. *Phys. Chem. Chem. Phys.* **2012**, *14*, 5090.
(21) Atkin, R.; Borisenko, N.; Drüschler, M.; El Abedin, S. Z.; Endres, F.; Hayes, R.; Huber, B.; Roling, B. An in situ STM/AFM and impedance spectroscopy study of the extremely pure 1-butyl-1-methylpyrrolidinium tris (pentafluoroethyl) trifluorophosphate/Au(111) interface: potential dependent solvation layers and the herringbone reconstruction. *Phys. Chem. Chem. Phys.* **2011**, *13*, 6849.
(22) Lockett, V.; Horne, M.; Sedev, R.; Rodopoulos, T.; Ralston, J. Differential capacitance of the double layer at the electrode/ionic liquids interface. *Phys. Chem. Chem. Phys.* **2010**, *12*, 12499.
(23) Gore, T. R.; Bond, T.; Zhang, W.; Scott, R. W.; Burgess, I. J. Hysteresis in the measurement of double-layer capacitance at the gold−ionic liquid interface. *Electrochem. Commun.* **2010**, *12*, 1340.
(24) Drüschler, M.; Huber, B.; Passerini, S.; Roling, B. Hysteresis effects in the potential-dependent double layer capacitance of room temperature ionic liquids at a polycrystalline platinum interface. *J. Phys. Chem. C* **2010**, *114*, 3614.
(25) Lockett, V.; Sedev, R.; Ralston, J.; Horne, M.; Rodopoulos, T. Differential capacitance of the electrical double layer in imidazolium-based ionic liquids: Influence of potential, cation size, and temperature. *J. Phys. Chem. C* **2008**, *112*, 7486.
(26) Zhou, W.; Xu, Y.; Ouchi, Y. Hysteresis effects in the in situ SFG and differential capacitance measurements on metal electrode/ionic liquids interface. *ECS Trans.* **2013**, *50*, 339.
(27) Zhou, W.; Inoue, S.; Iwahashi, T.; Kanai, K.; Seki, K.; Miyamae, T.; Kim, D.; Katayama, Y.; Ouchi, Y. Double layer structure and adsorption/desorption hysteresis of neat ionic liquid on Pt electrode surface—an in-situ IR-visible sum-frequency generation spectroscopic study. *Electrochem. Commun.* **2010**, *12*, 672.
(28) Motobayashi, K.; Minami, K.; Nishi, N.; Sakka, T.; Osawa, M. Hysteresis of potential-dependent changes in ion density and structure of an ionic liquid on a gold electrode: in situ observation by surface-enhanced infrared absorption spectroscopy. *J. Phys. Chem. Lett.* **2013**, *4*, 3110.
(29) Black, J.; Walters, D.; Labuda, A.; Feng, G.; Hillesheim, P. C.; Dai, S.; Cummings, P. T.; Kalinin, S. V.; Proksch, R.; Balke, N. Bias-dependent molecular-level structure of electrical double layer in ionic liquid on graphite. *Nano Lett.* **2013**, DOI: 10.1021/nl4031083.
(30) Mezger, M.; Schröder, H.; Reichert, H.; Schramm, S.; Okasinski, J. S.; Schöder, S.; Honkimäki, V.; Deutsch, M.; Ocko, B. M.; Ralston, J. Molecular layering of fluorinated ionic liquids at a charged sapphire(0001) surface. *Science* **2008**, *322*, 424.
(31) Yamamoto, R.; Morisaki, H.; Sakata, O.; Shimotani, H.; Yuan, H.; Iwasa, Y.; Kimura, T.; Wakabayashi, Y. External electric field dependence of the structure of the electric double layer at an ionic liquid/Au interface. *Appl. Phys. Lett.* **2012**, *101*, 053122.
(32) Zhou, H.; Rouha, M.; Feng, G.; Lee, S. S.; Docherty, H.; Fenter, P.; Cummings, P. T.; Fulvio, P. F.; Dai, S.; McDonough, J.; Gogotsi, Y. Nanoscale perturbations of room temperature ionic liquid structure at charged and uncharged interfaces. *ACS Nano* **2012**, *6*, 9818.
(33) Zhou, H.; Ganesh, P.; Presser, V.; Wander, M. C.; Fenter, P.; Kent, P. R.; Jiang, D.-e.; Chialvo, A. A.; McDonough, J.; Shuford, K. L.; Gogotsi, Y. Understanding controls on interfacial wetting at epitaxial graphene: Experiment and theory. *Phys. Rev. B* **2012**, *85*, 035406.
(34) Fenter, P.; Kerisit, S.; Raiteri, P.; Gale, J. D. Is the calcite−water interface understood? Direct comparisons of molecular dynamics

simulations with specular X-ray reflectivity data. *J. Phys. Chem. C* **2013**, *117*, 5028.
(35) Wang, J.; Davenport, A. J.; Isaacs, H. S.; Ocko, B. Surface charge-induced ordering of the Au(111) surface. *Science* **1992**, *255*, 1416.
(36) Cheng, L.; Fenter, P.; Nagy, K. L.; Schlegel, M. L.; Sturchio, N. C. Molecular-scale density oscillations in water adjacent to a mica surface. *Phys. Rev. Lett.* **2001**, *87*, 156103.
(37) Uysal, A.; Chu, M.; Stripe, B.; Timalsina, A.; Chattopadhyay, S.; Schlepütz, C. M.; Marks, T. J.; Dutta, P. What X-rays can tell us about the interfacial profile of water near hydrophobic surfaces. *Phys. Rev. B* **2013**, *88*, 035431.
(38) Yu, C. J.; Richter, A. G.; Datta, A.; Durbin, M. K.; Dutta, P. Observation of molecular layering in thin liquid films using X-ray reflectivity. *Phys. Rev. Lett.* **1999**, *82* (11), 2326.
(39) Hayes, R.; Warr, G. G.; Atkin, R. At the interface: solvation and designing ionic liquids. *Phys. Chem. Chem. Phys.* **2010**, *12*, 1709.
(40) Miller, J. R.; Outlaw, R.; Holloway, B. Graphene double-layer capacitor with ac line-filtering performance. *Science* **2010**, *329*, 1637.
(41) Wu, Z. S.; Parvez, K.; Feng, X.; Müllen, K., Graphene-based in-plane micro-supercapacitors with high power and energy densities. *Nat. Commun.* **2013**, *4*, DOI: 10.1038/ncomms3487.
(42) Fister, T. T.; Long, B. R.; Gewirth, A. A.; Shi, B.; Assoufid, L.; Lee, S. S.; Fenter, P. Real-time observations of interfacial lithiation in a metal silicide thin film. *J. Phys. Chem. C* **2012**, *116*, 22341.
(43) Fenter, P. A. X-ray reflectivity as a probe of mineral-fluid interfaces: A user guide. *Rev. Mineral. Geochem.* **2002**, *49*, 149.
(44) Emtsev, K. V.; Bostwick, A.; Horn, K.; Jobst, J.; Kellogg, G. L.; Ley, L.; McChesney, J. L.; Ohta, T.; Reshanov, S. A.; Röhrl, J. Towards wafer-size graphene layers by atmospheric pressure graphitization of silicon carbide. *Nat. Mater.* **2009**, *8*, 203.
(45) Meunier, V.; Kalinin, S. V.; Shin, J.; Baddorf, A. P.; Harrison, R. J. Quantitative analysis of electronic properties of carbon nanotubes by scanning probe microscopy: from atomic to mesoscopic length scales. *Phys. Rev. Lett.* **2004**, *93*, 246801.
(46) Borodin, O. Polarizable force field development and molecular dynamics simulations of ionic liquids. *J. Phys. Chem. B* **2009**, *113*, 11463.
(47) Lindahl, E.; Hess, B.; van der Spoel, D. GROMACS 3.0: A package for molecular simulation and trajectory analysis. *J Mol. Model.* **2001**, *7*, 306.
(48) Yeh, I. C.; Berkowitz, M. L. Ewald summation for systems with slab geometry. *J. Chem. Phys.* **1999**, *111*, 3155.
(49) Hess, B.; Bekker, H.; Berendsen, H. J. C.; Fraaije, J. G. E. M. LINCS: A linear constraint solver for molecular simulations. *J. Comput. Chem.* **1997**, *18*, 1463.
(50) Magnussen, O. M.; Ocko, B. M.; Regan, M. J.; Penanen, K.; Pershan, P. S.; Deutsch, M. X-ray reflectivity measurements of surface layering in liquid mercury. *Phys. Rev. Lett.* **1995**, *74*, 4444.
(51) Perkin, S.; Salanne, M.; Madden, P.; Lynden-Bell, R. Is a Stern and diffuse layer model appropriate to ionic liquids at surfaces? *Proc. Natl. Acad. Sci. U.S.A.* **2013**, *110*, E4121.
(52) Gebbie, M. A.; Valtiner, M.; Banquy, X.; Henderson, W. A.; Israelachvili, J. N. Reply to Perkin et al.: Experimental observations demonstrate that ionic liquids form both bound (Stern) and diffuse electric double layers. *Proc. Natl. Acad. Sci. U.S.A.* **2013**, *110*, E4122.
(53) Drüschler, M.; Huber, B.; Roling, B. On capacitive processes at the interface between 1-ethyl-3-methylimidazolium tris-(pentafluoroethyl) trifluorophosphate and Au(111). *J. Phys. Chem. C* **2011**, *115*, 6802.